IEEE Access
Multidisciplinary | Rapid Review | Open Access Journal

Received November 28, 2016, accepted December 10, 2016, date of publication December 14, 2016, date of current version February 25, 2017.

Digital Object Identifier 10.1109/ACCESS.2016.2639517

Optimization of the Overall Success Probability of the Energy Harvesting Cognitive Wireless Sensor Networks

MATEEN ASHRAF[1], ADNAN SHAHID[2], (Member, IEEE), JU WOOK JANG[3], AND KYUNG-GEUN LEE[1]

[1]Sejong University, seoul 143-747, South Korea
[2]Ghent University, Ghent 9052, Belgium
[3]Sogang University, seoul 04107, South Korea

Corresponding author: Kyung-Geun Lee (kglee@sejong.ac.kr)

This work was supported by the Institute for Information and Communications Technology Promotion by the Korean Government (MSIP) under Grant B0126-16-1051.

ABSTRACT Wireless energy harvesting can improve the performance of cognitive wireless sensor networks (WSNs). This paper considers radio frequency (RF) energy harvesting from transmissions in the primary spectrum for cognitive WSNs. The overall success probability of the energy harvesting cognitive WSN depends on the transmission success probability and energy success probability. Using the tools from stochastic geometry, we show that the overall success probability can be optimized with respect to: 1) transmit power of the sensors; 2) transmit power of the primary transmitters; and 3) spatial density of the primary transmitters. In this context, an optimization algorithm is proposed to maximize the overall success probability of the WSNs. Simulation results show that the overall success probability and the throughput of the WSN can be significantly improved by optimizing the aforementioned three parameters. As RF energy harvesting can also be performed indoors, hence, our solution can be directly applied to the cognitive WSNs that are installed in smart buildings.

INDEX TERMS RF energy harvesting, success probability, spectrum sharing, stochastic geometry, wireless sensor networks.

I. INTRODUCTION

Smart buildings will comprise the major portion of the smart cities of the future. WSNs are widely used for surveillance and control purposes of the smart buildings [1]. The sensors usually sense some physical activity in the surrounding environment and report it to the information sink (IS). The frequency band that is used by the sensors is also used simultaneously by some other applications (e.g. wifi). This results in interference at the receiving end. The other major problem is linked with the batteries of the sensors. The process of reporting information to the IS can exhaust the batteries of the sensors quite quickly. Replacing the batteries may not be feasible due to the physical location of the sensors or due to the dependence of the human activity for performing battery replacement. The problem of battery exhaustion can be solved by using wireless energy harvesting. The study of wireless energy harvesting for communication networks is gaining much interest from the research community [2]–[7]. The main reason for these research efforts is the vast availability of the energy present in the ambient environment. The main advantages of energy harvesting are the decrease in the carbon emission in the environment, improvement in the life time of the network and the ability to provide power to those devices that cannot be charged through fixed power outlets [5]. Wireless energy harvesting in communication networks can be performed from renewable sources [6] e.g. wind, vibrations, solar, thermoelectric or from ambient radio frequency transmissions [2]–[5], [7]. Energy harvesting from renewable sources may not be reliable due to the dependence on the weather conditions, time of day and physical location of the energy harvesting device. In particular, energy harvesting from solar energy can only be performed during the day time.

The spectrum sharing with energy harvesting nodes is discussed in [8]–[13]. In [8], the cognitive relay selection is discussed, and the exact outage performance of the cognitive

network is found. However, they have assumed that the distance between cognitive nodes and the primary nodes is same for all the cognitive relay nodes. Liu et. al. in [9] have analyzed the performance of cognitive network when time splitting protocol is used for energy harvesting at the cognitive relay. Interference effects from primary transmitters to cognitive receivers are analyzed in their work. Spectrum sharing based on splitting of the spectrum for primary and cognitive radio is discussed in [10]. The cognitive radio performs relaying operations for the primary users on one part of the primary spectrum while the cognitive radio uses the other part of the spectrum to transmit its own information to the cognitive receiver. A similar approach is discussed in [11] where power splitting is used at the cognitive relay instead of bandwidth splitting. Optimal power splitting at the cognitive relay is found with the help of biconvex optimization for maximizing the sum of primary and cognitive data rates. In [12] and [13] the authors have used stochastic geometry to evaluate the performance of the energy harvesting D2D cognitive communication. In [12], dedicated RF power transmitters are considered for powering the D2D devices while in [13] the RF energy harvesting at the D2D devices is performed from the transmissions of the primary network.

A. RELATED WORK AND MOTIVATION

The existing work on energy harvesting WSN can be categorized into the following two types (i) energy harvesting from renewable sources (solar, wind, etc.) and (ii) energy harvesting from ambient radio frequency transmissions [14]. WSNs relying on renewable sources are discussed in [15]–[20]. A framework for investigating the performance of WSNs with solar energy harvesting is presented in [15]. The authors have considered the hardware architecture and software design for a prototype of a WSN. An energy management system to efficiently utilize the energy harvested from solar radiations is provided in [16]. An energy storage device assisted by a solar energy harvesting system is presented in [17]. The system uses battery power when the weather is overcast or rainy, and it resorts to solar radiations when sunshine is sufficient. Different sleep and wake-up strategies for solar powered WSNs are provided in [18]. The optimization of the strategies is performed with the help of Markov chain queuing models. Energy harvesting from human bodies is discussed in [19] and [20]. Energy harvesting from human body temperature for WSNs was discussed in [19]. In [20], the Piezo electric effect is used to harvest the energy from human body motions to power wireless sensors. In all of the above works spectrum sharing with a primary network is not considered.

The use of RF energy harvesting for WSNs is discussed in [21]–[28]. In [21], the technical aspects including the RF energy harvesting and delivery of the RF energy harvesting WSNs were reviewed. It is shown that RF energy harvesting can be a preferred solution for powering small sized sensors. A distributed medium access protocol, named RF-MAC, for RF energy harvesting sensors is proposed in [22]. The protocol is shown to achieve a gain of about 300% in terms of throughput and 100% in terms of average harvested energy. An efficient and high gain antenna design for RF energy harvesting WSNs is proposed in [23]. Optimal mode selection for battery assisted RF energy harvesting cognitive WSN is provided in [24]. An optimal policy is developed to find a tradeoff between the harvested energy and the throughput of the WSN. The distribution of the harvested energy from a fixed number of energy transmitters is found in [25]. It is shown that the harvested voltages over the network follow Rayleigh distribution. In cases when sensors are equipped with energy storage devices it is possible to accumulate energy over a number of time slots and hold transmission until the harvested energy is above a given threshold. In this case the performance of the WSN in terms of update age and update cycle is investigated in [26]. However, they have not considered the spectrum sharing in their work. In [27] the performance of energy harvesting WSN is analyzed in presence of the interference from the primary network. However, they have assumed that energy is harvested from single primary transmitter and the interference is also caused by a single primary transmitter. In a practical scenario the sensors maybe distributed according to some point process in the environment. Mekikis *et al.* [28] have considered random distribution of sensors and derived the analytical expression for the probability of successful communication between two types of sensors. However, in their research, they have considered communication among sensors only and not the spectrum sharing with the primary network. In summary, none of the above work jointly discuss the performance of the primary network and the WSN. The transmit powers of the primary network and sensor can affect the performance of the whole system due to the interference caused among networks to one another.

In this work, we have optimized the performance of the energy harvesting cognitive WSN under the constraint that the primary network coverage is above a given threshold. The sensors use the downlink spectrum of the primary transmissions for reporting their sensed information to the IS. The effect of transmit powers of the primary transmitters, sensors and the density of the primary transmitters on the performance of the WSN is analyzed. We have considered RF energy harvesting for sensors. The individual sensors harvest energy from RF transmissions in the primary spectrum. The reasons for choosing RF energy harvesting are as follows. First, RF energy is controllable in comparison to other renewable sources like solar, wind, etc. Secondly, RF energy harvesting can be performed in indoor environments as well as outdoor environments. Third, the energy harvesting efficiency for an RF case is much higher than the harvesting efficiencies for other energy sources [29]. Further, our work is different from existing works in that we have considered the communicating entities to be spatially distributed according to the Poisson point process (PPP). Therefore, our results are based on averaging over all the possible distances between the communicating entities. The main contribution of this paper are summarized below:

- We have analytically shown that the performance of the WSN in terms of the overall success probability can be optimized with respect to the transmit power of the primary transmitters, sensors and spatial density of the primary transmitters.
- An optimization algorithm is proposed to optimize the performance of the WSN with respect to the transmit power of the primary transmitters, sensors and the density of the primary transmitters with the constraint that primary network coverage remains higher than a given threshold.
- Simulations are carried out to show the improvement in the overall success probability and throughput of the WSN after performing the optimization with respect to transmit powers and density of the primary transmitters.

The paper is organized as follows. Section 2 discusses the system model and the relevant assumptions. The performance evaluation is carried out in Section 3. The simulation results are discussed in Section 4. Finally, conclusions are provided in Section 5.

II. SYSTEM MODEL AND ASSUMPTIONS

In the following we describe the spatial distribution, channel model, energy harvesting, spectrum allocation and performance metric in detail. The important parameters that are used in the rest of the paper are also provided in Table I.

TABLE 1. System parameters.

Parameter	Description
P_s	sensor transmit power
P_p	primary transmit power
α	Path loss exponent
λ_s	density of the sensors
λ_p	density of the primary transmitters
Φ	Poisson point process of primary transmitters
Φ_s	Poisson point process of sensors

A. SPATIAL DISTRIBUTION

In the system model, we assume that primary transmitters are internet access points (APs) e.g. wifi routers installed within an indoor environment. The spatial distribution of APs is assumed to follow a two dimensional homogeneous Poisson point process (2D-HPPP) with density λ_p. The wireless sensors are also assumed to be spatially distributed with 2D-HPPP with density λ_s. It is assumed that sensors report their sensed information to the nearest IS. The ISs are also assumed to be spatially distributed with density λ_c. The PPPs of the AP's, IS's and sensors are denoted by Φ, Φ_c and Φ_s respectively. It is assumed that Φ, Φ_c and Φ_s are mutually independent. A pictorial representation of the system model is provided in Fig. 1. Any primary device or sensor connects to the corresponding nearest AP and IS according to the voronoi tessellation to maximize the average received power. The transmit power level of the APs is P_p and that of the sensors is P_s.

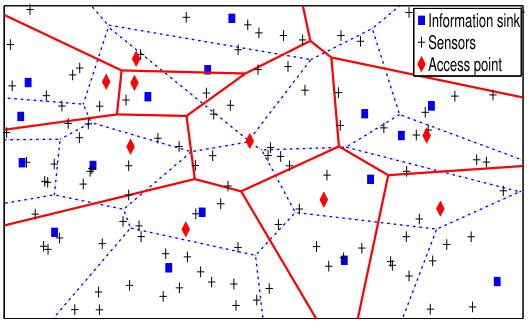

FIGURE 1. System model comprising of sensors, information sinks and access points.

B. CHANNEL MODEL

The channels are assumed to be quasi static. This means the channels remain fixed over a given time slot; however, the channels can assume different values at different time slots. The channel among any two communicating entities is affected by small scale fading as well as the path loss. The small scale fading is assumed to follow exponential distribution with parameter 1, and the path loss for a propagation distance d is $d^{-\alpha}$ where α is the path loss exponent. It is noted in [31] that for obstructed indoor environments the value of the path loss exponent varies from $4-6$.

C. ENERGY HARVESTING

The APs, primary receivers and ISs are assumed to be operating at fixed power supplies. However, the sensors rely on wireless energy harvesting for their transmissions. The sensors do not have any energy storage device and the energy harvested in the current time slot can not be used for future time slots [13]. In particular, the sensors harvest energy from the concurrent transmissions from the APs and other sensors. This means that the number of energy transmitters that are available for the energy harvesting are equal to the number of transmissions in the shared spectrum. In the event that the harvested energy is above a given threshold in a given time slot then sensor will transmit [13] its sensed information to the nearest IS. This implies that the overall success probability of the sensor network depends on the cumulative distribution function of the harvested energy in a time slot.

D. SPECTRUM USAGE

All the APs use the frequency spectrum with a frequency reuse factor of 1 to maximize the spectrum efficiency. The sensors use the same spectrum as used by the APs for downlink communication. Therefore, the transmissions from the sensors cause interference to the primary receivers in the downlink. The interference can cause reduction in the success probability of the APs downlink communication. We assume that there is a minimum success probability, P^p_{suc}, and the success probability of the AP downlink should not be less than P^p_{suc} due to the interference from the concurrent sensor transmissions and neighboring APs transmissions. The success probability constraint on the AP transmission

is met by imposing a constraint on the maximum spectrum access probability of the sensors. Therefore, according to the coloring theorem, the PPP of the sensors that can access the spectrum for a given spectrum access probability p_{SA} is another PPP (Φ_{ts}) with density $\lambda_s p_{SA}$. The network performance is assumed to be interference limited and therefore noise is not considered in the analysis to simplify the notation.

E. PERFORMANCE METRIC

The performance metric in this paper is the overall success probability of the sensor communications under the constraint that the success probability of the primary communication is higher than P^p_{suc}. The overall success probability of WSN depends on two factors. First, the probability that the received SIR of a typical sensor at its nearest IS is higher than a given threshold and secondly the probability that a typical sensor has harvested enough energy to be able to transmit.

III. PERFORMANCE ANALYSIS

First, we find the maximum spectrum access probability for the sensor for a given success probability constraint on the primary network. After that, we analyze the secondary performance. To find the signal to interference ratio (SIR) of a particular primary receiver we use the Sliynyak theorem and place the primary receiver at the origin. The received signal at the primary receiver is the sum of the desired signal and the interference from the primary transmissions and sensor transmissions. Therefore, the SIR for a particular primary receiver can be written as

$$\gamma_p = \frac{P_p g_0 x_0^{-\alpha}}{P_p \sum_{i\in\Phi\setminus 0} g_i x_i^{-\alpha} + P_s \sum_{j\in\Phi_{ts}} h_j y_j^{-\alpha}}, \tag{1}$$

where $g_i(h_j)$ capture the small scale fading effect of the transmissions from $i(j)$-th primary (secondary) transmitter, $x_i(y_j)$ is the distance from the $i(j)$-th primary (secondary) transmitter, $\Phi(\Phi_{ts})$ denote the PPP of the primary (secondary) transmitters. To find the maximum value of p_{SA} which will make sure that success probability of the primary receiver for a given SIR threshold T_p is greater than P^p_{suc}, we solve the following equation [32]

$$P_{suc} = \int_0^\infty Pr\left[\gamma_p \geq T_p | x_0\right] p_{\mathbf{x_0}}(x_0) dx_0 \geq P^p_{suc}, \tag{2}$$

where $p_{\mathbf{x_0}}(x_0) = 2\pi\lambda_p x_0 e^{-\pi\lambda_p x_0^2}$ is the probability density function of the distance of a typical primary receiver to its nearest primary transmitter [30]. First, we find the inner probability then we will integrate it over all possible values of $\mathbf{x_0}$. Since, the small scale fading is distributed exponentially with parameter 1 therefore we can write the inner probability as [32]

$$Pr\left[\gamma_p \geq T_p \middle| x_0\right] = \underbrace{E_{\mathbf{g_i},\mathbf{x_i}}\left[e^{-T_p x_0^\alpha \sum_{i\in\Phi\setminus 0} g_i x_i^{-\alpha}}\right]}_{A} \times \underbrace{E_{\mathbf{h_j},\mathbf{y_j}}\left[e^{-T_p x_0^\alpha \frac{P_s}{P_p} \sum_{j\in\Phi_{ts}} h_j y_j^{-\alpha}}\right]}_{B}, \tag{3}$$

where $E_X[.]$ denotes the expectation operation over random variable X. Now, using the independence between small scale fading and the spatial distribution we can write [32]

$$A = E_{\mathbf{x_i}}\left[\prod_{i\in\Phi\setminus 0} E_{\mathbf{g_i}}\left[e^{-T_p x_0^\alpha g_i x_i^{-\alpha}}\right]\right]. \tag{4}$$

Using the fact that all the g_i's are i.i.d. and probability generating functional (PGFL) [32] we can write

$$\begin{aligned} A &= E_{\mathbf{x_i}}\left[\prod_{i\in\Phi\setminus 0} E_{\mathbf{g_i}}\left[e^{-T_p x_0^\alpha g_i x_i^{-\alpha}}\right]\right] \\ &= e^{-2\pi\lambda_p \int_{x_0}^\infty (1 - E_g[e^{-T_p x_0^\alpha g x^{-\alpha}}]) x dx}, \end{aligned} \tag{5}$$

Since g is exponentially distributed with mean 1 therefore $E_g[e^{-T_p x_0^\alpha g x^{-\alpha}}] = \frac{1}{1+T_p x_0^\alpha x^{-\alpha}}$ and we can write

$$A = e^{-2\pi\lambda_p \int_{x_0}^\infty \left(\frac{T_p x_0^\alpha x^{-\alpha}}{1+T_p x_0^\alpha x^{-\alpha}}\right) x dx}, \tag{6}$$

here the lower limit is x_0 because the nearest primary interferer has a distance $> x_0$. After doing some mathematical manipulations as mentioned in appendix we can write

$$A = e^{-\pi\lambda_p x_0^2 \vartheta(T_p)}, \tag{7}$$

where $\vartheta(T_p) = \frac{2T_p}{\alpha-2} {}_2F_1(1, \frac{\alpha-2}{\alpha}; \frac{2\alpha-2}{\alpha}; -T_p)$ and ${}_2F_1(u, v; w; x)$ is the Gauss Hypergeometric function. In a similar way by using the independence between h_j, y_j and using the PGFL we can write

$$B = e^{-2\pi\lambda_s p_{SA} \int_0^\infty \left(\frac{T_p \frac{P_s}{P_p} x_0^\alpha y^{-\alpha}}{1+T_p \frac{P_s}{P_p} x_0^\alpha y^{-\alpha}}\right) y dy}, \tag{8}$$

where the lower limit is 0 because the secondary interferers can have any distance from 0 to ∞. After carrying out integration as mentioned in appendix we can write

$$B = e^{-\pi\lambda_s p_{SA} (T_p \frac{P_s}{P_p})^{\frac{2}{\alpha}} x_0^2 \Gamma(\frac{\alpha-2}{\alpha})\Gamma(\frac{\alpha+2}{\alpha})}, \tag{9}$$

where $\Gamma(x)$ is the Gamma function of x. Using (9), (7) and (3) we can write (2) as follows

$$P_{suc} = \int_0^\infty e^{-\pi\lambda_p x_0^2 \vartheta(T_p) - \pi\lambda_s p_{SA} (T_p \frac{P_s}{P_p})^{\frac{2}{\alpha}} x_0^2 \Gamma(\frac{\alpha-2}{\alpha})\Gamma(\frac{\alpha+2}{\alpha}) - \pi\lambda_p x_0^2} 2\pi\lambda_p x_0 dx_0. \tag{10}$$

After carrying out the integration with respect to x_0 we can write

$$P_{suc} = \frac{\lambda_p}{\lambda_p \vartheta(T_p) + \left(T_p \frac{P_s}{P_p}\right)^{\frac{2}{\alpha}} \frac{2}{\alpha}\Gamma(\frac{2}{\alpha})\Gamma(\frac{\alpha-2}{\alpha})\lambda_s p_{SA} + \lambda_p} \tag{11}$$

and the corresponding value of $p_{SA,max}$ can be obtained by putting (11) in (2) as follows

$$p_{SA,max} = \frac{\alpha^2 \kappa^{\frac{2}{\alpha}} \left[P^p_{suc}(\vartheta(T_p)+1) - 1\right]}{4\Gamma(\frac{2}{\alpha})\Gamma(-\frac{2}{\alpha}) P^p_{suc} T_p^{\frac{2}{\alpha}}}, \tag{12}$$

where $\kappa = \left(\frac{\lambda_p^{\frac{\alpha}{2}} P_p}{\lambda_s^{\frac{\alpha}{2}} P_s}\right)$. It is to be emphasized here that the density of the sensors that can access the spectrum is assumed to be $p_{SA}\lambda_s$. Now we analyze the performance of the sensor network. As discussed above the overall success probability of the sensor network depends on two factors. First, the ability of the sensor to communicate successfully with its nearest IS in the event that the sensor transmits. This factor is calculated to account for the channel imperfections and interference effect when a sensor transmits. Second, the ability of the sensor to harvest enough energy from the transmissions in the primary frequency band to be able to transmit. This factor is calculated to account for the uncertainty in the ability of the sensor to transmit due to random harvested energy and the condition that a sensor will transmit only if the harvested power is greater than a given threshold. We denote the first factor as the transmission success probability and the second factor will be called energy success probability. By multiplying these factors we make sure that overall success probability measures the probability of the event that a sensor is able to transmit and its transmitted signal is correctly decoded at the IS. The transmission success probability of typical sensor can be computed with the help of the received SIR at the nearest IS. By using the Slivnyak theorem and placing the nearest IS at the origin the received SIR at the IS for a typical sensor in Φ_s can be written as

$$\gamma_s = \frac{P_s h_0 y_0^{-\alpha}}{P_p \sum_{i\in\Phi} g_i x_i^{-\alpha} + P_s \sum_{j\in\Phi_{ts}\setminus 0} h_j y_j^{-\alpha}}. \tag{13}$$

The transmission success probability of the sensor for a given SIR threshold T_s is given as follows [32]

$$P_{tr,s} = \int_0^\infty Pr\left(\gamma_s > T_s | y_0\right) p_{\mathbf{y_0}}(y_0) dy_0, \tag{14}$$

where $p_{\mathbf{y_0}}(y_0) = 2\pi\lambda_s y_0 e^{-\pi\lambda_s y_0^2}$ is the probability density function of the distance of a typical sensor to its nearest IS. The inner probability can be written as follows

$$\begin{aligned} &Pr\left(\gamma_s > T_s | y_0\right) \\ &= E_{\mathbf{g_i},\mathbf{x_i},\mathbf{h_j},\mathbf{y_j}}\left[\frac{P_s h_0 y_0^{-\alpha}}{P_p \sum_{i\in\Phi} g_i x_i + P_s \sum_{j\in\Phi_{ts}\setminus 0} h_j y_j^{-\alpha}} > T_s\right]. \end{aligned} \tag{15}$$

Since, h_0 follows an exponential distribution with mean 1 therefore we can write

$$\begin{aligned} &Pr\left(\gamma_s > T_s | y_0\right) \\ &= E_{\mathbf{g_i},\mathbf{x_i},\mathbf{h_i},\mathbf{y_i}}\left[e^{-T_s y_0^{\alpha}\frac{P_p}{P_s}\sum_{i\in\Phi} g_i x_i - T_s y_0^{\alpha}\sum_{j\in\Phi_{ts}\setminus 0} h_j y_j^{-\alpha}}\right]. \end{aligned} \tag{16}$$

By using the independence of h_j, g_i, x_i and y_j we can write the above probability as follows

$$\begin{aligned} Pr\left(\gamma_s > T_s | y_0\right) = &\underbrace{E_{\mathbf{g_i},\mathbf{x_i}}\left[e^{-T_s y_0^{\alpha}\frac{P_p}{P_s}\sum_{i\in\Phi} g_i x_i}\right]}_{C} \\ &\times \underbrace{E_{\mathbf{h_i},\mathbf{y_i}}\left[e^{-T_s y_0^{\alpha}\sum_{j\in\Phi_{ts}\setminus 0} h_j y_j^{-\alpha}}\right]}_{D}. \end{aligned} \tag{17}$$

Following the same line of reasoning, the independence between h_j, g_i, x_i, y_j and PGFL, that was used to obtain A in (7) and B in (9) we can obtain the values of C and D as follows

$$\begin{aligned} C &= e^{-2\pi\lambda_p \int_0^\infty \frac{T_s y_0^{\alpha}\frac{P_p}{P_s} x^{-\alpha}}{1+T_s y_0^{\alpha}\frac{P_p}{P_s} x^{-\alpha}} x dx}, \\ D &= e^{-2\pi p_{SA,max}\lambda_s \int_{y_0}^\infty \frac{T_s y_0^{\alpha} y^{-\alpha}}{1+T_s y_0^{\alpha} y^{-\alpha}} y dy}. \end{aligned} \tag{18}$$

The mathematical form of C and D is similar to the form of B and A, respectively. Therefore, same steps that were used to simplify A and B can be used to simplify C and D also. After performing the simplification mentioned in appendix we can write C and D as follows

$$\begin{aligned} C &= e^{-\pi\lambda_p\left(\frac{T_s P_p}{P_s}\right)^{\frac{2}{\alpha}} y_0^2 \Gamma(1+\frac{2}{\alpha})\Gamma(1-\frac{2}{\alpha})}, \\ D &= e^{-\pi p_{SA,max}\lambda_s y_0^2 \vartheta(T_s)}. \end{aligned} \tag{19}$$

Using (19), (17) and (14) we can write the transmission success probability as

$$\begin{aligned} P_{tr,s} = &\int_0^\infty e^{-\pi\lambda_p\left(\frac{T_s P_p}{P_s}\right)^{\frac{2}{\alpha}} y_0^2 \Gamma(1+\frac{2}{\alpha})\Gamma(1-\frac{2}{\alpha}) - \pi p_{SA,max}\lambda_s y_0^2 \vartheta(T_s)} \\ &\times e^{-\pi\lambda_s y_0^2} 2\pi\lambda_s y_0 dy_0. \end{aligned} \tag{20}$$

After carrying out integration with respect to y_0 we can write the $P_{tr,s}$ as follows

$$P_{tr,s} = \frac{1}{1 + p_{SA,max}\vartheta(T_s) + \kappa^{\frac{2}{\alpha}}\Gamma(1+\frac{2}{\alpha})\Gamma(1-\frac{2}{\alpha}) T_s^{\frac{2}{\alpha}}}. \tag{21}$$

After putting (12) in (21) we can easily observe that for fixed values of $\lambda_s, \lambda_p, P_p$ the value of $P_{tr,s}$ increases with increasing P_s. Although the interference contribution due to the increase in P_s increases however according to (21) the increase in interference is outweighed by the increase in received signal power. Similarly, it can be observed that $P_{tr,s}$ decreases with increasing P_p and λ_p. This is because increasing λ_p and P_p increases the interference at the IS thereby decreasing $P_{tr,s}$.

Now, we find the energy success probability that is the probability that the harvested power at a typical sensor is greater than a given threshold P_s. First, we consider the case when energy harvesting is performed from AP's transmission only. After that we show the energy success probability for the case when energy harvesting is performed from the AP's

transmissions as well as sensors transmissions in the primary band. This is because we have considered the interference from the sensors while computing the success probability of the primary transmissions. In our energy harvesting model we have assumed that energy harvesting is performed in the same frequency band that is used for transmission of the sensed information. We have assumed, widely used, harvest then transmit protocol. In this protocol [13] it is assumed that the RF energy harvesting and DC conversion circuits of a sensor are activated only when the available power in the time-slot is at least equal to a given threshold. There is no energy storage assumed where a sensor can save extra energy for the future time slots. The same assumption for energy harvesting are used in [13] where energy harvesting is performed in the frequency band $[c_1, c_2 \cdots c_d, \cdots c_{|C|}]$ and c_d band is used by the D2D device to transmit its own information. To calculate the energy success probability we note that the power available at any given time slot is proportional to the received powers from all the APs in Φ. Mathematically, we can write the received power in any time slot as follows [33]

$$P_h = \nu \sum_{i\in\Phi} P_p g_i x_i^{-\alpha}, \tag{22}$$

where $0 < \nu \leq 1$ is the energy harvesting efficiency. The energy success probability is given as follows

$$P_{e,s} = Pr(P_h > P_s) = Pr\left(\nu \sum_{i\in\Phi} P_p g_i x_i^{-\alpha} > P_s\right). \tag{23}$$

The Laplace transform of the probability density function of $\nu \sum_{i\in\Phi} P_p g_i x_i^{-\alpha}$ can be written as [33]

$$\mathcal{L}_{P_h} = e^{-\frac{2\pi^2 \lambda_p (P_p \nu s)^{\frac{2}{\alpha}}}{\alpha \sin(\frac{2\pi}{\alpha})}}, \tag{24}$$

and the corresponding $Pr(P_h > P_s)$ can be found using the complex inversion integral formula for Laplace transforms and the proper Bromwich contour [33]. After mathematical simplifications the complementary cumulative distribution function (CCDF) of the P_h is given as follows [33]

$$P_{e,s} = \int_0^\infty \frac{1}{\pi x} e^{-xP_s - \frac{2\pi^2 \lambda_p \left(\nu x P_p\right)^{\frac{2}{\alpha}}}{\alpha \tan\left(\frac{2\pi}{\alpha}\right)}} \sin\left(\frac{2\pi^2 \lambda_p \left(\nu x P_p\right)^{\frac{2}{\alpha}}}{\alpha}\right) dx. \tag{25}$$

Although it is easy to solve the above expression numerically however it is difficult to find a close form expression for general values of α. For $\alpha = 4$ we can obtain the close form expression as given below

$$P_{e,s}|_{\alpha=4} = 1 - erfc\left(\frac{\pi^2 \nu^{\frac{1}{2}} \lambda_p P_p^{\frac{1}{2}}}{4 P_s^{\frac{1}{2}}}\right). \tag{26}$$

Now, we consider the case when energy harvesting is performed from AP transmissions as well as from sensors transmissions. We are considering sensor transmissions for energy harvesting because we have considered the impact of their transmissions while finding the success probability of the AP transmissions. In this case the harvested power is $P_{h,s} = \nu\left[\sum_{i\in\Phi} P_p g_i x_i^{-\alpha} + \sum_{j\in\Phi_{ts}} P_s h_j y_j^{-\alpha}\right]$ where the subscript s denote that sensor transmissions are also considered in energy harvesting. The corresponding Laplace transform of the probability density function of $P_{h,s}$ is given as follows [33]

$$\mathcal{L}_{P_{h,s}} = e^{-\frac{2\pi^2 (\nu s)^{\frac{2}{\alpha}}\left[\lambda_p P_p^{\frac{2}{\alpha}} + p_{SA,max}\lambda_s P_s^{\frac{2}{\alpha}}\right]}{\alpha \sin(\frac{2\pi}{\alpha})}}. \tag{27}$$

The corresponding probability that $P_{h,s}$ is greater than P_s can be obtained with the help of appendix B and is given below

$$P_{e,s}^S = \int_0^\infty \frac{1}{\pi x} e^{-xP_s - \frac{2\pi^2 (\nu x)^{\frac{2}{\alpha}} \chi}{\alpha \tan\left(\frac{2\pi}{\alpha}\right)}} \sin\left(\frac{2\pi^2 (\nu x)^{\frac{2}{\alpha}} \chi}{\alpha}\right) dx, \tag{28}$$

where $\chi = \lambda_p P_p^{\frac{2}{\alpha}} + p_{SA,max}\lambda_s P_s^{\frac{2}{\alpha}}$ and superscript S denotes that sensors transmissions are also considered for energy harvesting. The corresponding expression for $\alpha = 4$ can be found to be [33]

$$P_{e,s}^S|_{\alpha=4} = 1 - erfc\left(\frac{\pi^2}{4} \nu^{\frac{1}{2}} \left[\frac{\lambda_p P_p^{\frac{1}{2}}}{P_s^{\frac{1}{2}}} + p_{SA,max}\lambda_s\right]\right). \tag{29}$$

From this expression we can conclude that energy success probability decreases with increasing P_s for $\alpha = 4$ even if we consider energy harvesting from sensor transmissions. This is because $erfc(x)$ is decreasing function of x and $p_{SA,max}$ is inversely proportional to P_s. It can be easily deduced that the same trend will also follow for $\alpha > 4$ because for the same distances the propagation loss will increase and hence the available power for energy harvesting will decrease. This means that for the obstructed indoor environment ($4 \leq \alpha \leq 6$) the energy success probability decreases with increasing P_s whether energy harvesting from sensor transmissions is considered or not considered. It can be observed from (29) that the energy success probability increases with increasing λ_p and P_p. On the other hand it can be observed that energy success probability decreases with increasing value of P_s. The overall success probability of the sensor network can be written as the product of the energy success probability and transmission success probability as follows

$$P_{OA,s} = P_{tr,s} P_{e,s}^S, \tag{30}$$

where $P_{tr,s}$ is given in (21) and $P_{e,s}^S$ is provided in (28). The behavior of the transmission success probability with respect to λ_p, P_p and P_s was inverse to the behavior of energy success probability. Therefore, we can say that the overall success probability can be optimized with respect to P_s, P_p and λ_p.

A. REMARK

The above analysis is carried out on the basis of single frequency band. However in practical systems, every AP transmits over a number of frequency bands. The optimality with respect to the three parameters provides more degrees of freedom for network optimization as compared to when optimization can be performed only on the basis of one parameter. Further, with the collaboration among APs the value of λ_p and P_p can be adjusted for different frequency bands in order to improve the performance of the sensor network. In addition, in some cases it is possible that one or two of the (P_p, P_s, λ_p) parameters are fixed. In these situations the optimization can be performed on the remaining nonfixed parameters to enhance the performance of WSNs.

In Fig. 2 we have provided an optimization algorithm for maximizing the overall success probability of the sensor network with respect to λ_p, P_p and P_s. The value of $P_{OA,s}$ for any P_p, P_s and λ_P can be obtained from (30). Due to complexity of the optimization problem it is difficult to obtain close form expressions for λ_p^*, P_p^* and P_s^*. Therefore, the optimization can be performed numerically and stopping criteria can be based on the convergence of the maximized value. It can be observed that the complexity increases with decreasing the step sizes Δ_λ, Δ_P, Δ_{P_s}. The complexity can be reduced by compromising the performance of the system and changing the stopping criteria $P_{OA,s}^{stop}$ for the algorithm.

1: $[\lambda_{p,min} : \Delta_\lambda : \lambda_{p,max}] \rightarrow \lambda^p$
2: $[P_{p,min} : \Delta_P : P_{p,max}] \rightarrow P^p$
3: for $i = 1 : \text{Length}(\lambda^p)$
4: $\quad \lambda^p(i) \rightarrow \lambda_{p,i}$;
5: $\quad$ for $j = 1 : \text{Length}(P^p)$
6: $\quad\quad P^p(j) \rightarrow P_{p,j}$;
7: $\quad\quad$ Find the maximum value of $P_{OA,s}$ for $\lambda_p = \lambda_{p,i}$, $P_p = P_{p,j}$, $P_s \in [P_{s,min} : \Delta_{P_s} : P_{s,max}]$ and store the optimized value as $P_{OA,s}(\lambda_{p,i}, P_{p,j}, P^*_{s,i,j})$.
8: $\quad\quad$ if $P_{OA,c}(\lambda_{p,i}, P_{p,j}, P^*_{s,i,j}) \geq P_{OA,c}^{stop}$
9: $\quad\quad\quad$ {
10: $\quad\quad\quad\quad \lambda^*_{p,i} \rightarrow \lambda^*_p$;
11: $\quad\quad\quad\quad P^*_{p,j} \rightarrow P^*_p$;
12: $\quad\quad\quad\quad P^*_{s,i,j} \rightarrow P^*_s$;
13: $\quad\quad\quad\quad$ Break;
14: $\quad\quad\quad$ }
15: $\quad$ end
16: end
17: find the values of i^*, j^* for which $P_{OA,s}(\lambda_{p,i}, P_{p,j}, P^*_{s,i,j})$ is maximum.
18: Return: $\lambda^*_p = \lambda_p(i^*)$, $P^*_p = P_p(j^*)$ and $P^*_s = P^*_{s,i^*,j^*}$ as the optimum values.

FIGURE 2. Optimization algorithm for maximizing the overall success probability of sensor network.

It can be noted that if $P_{OA,s}^{stop}$ is less than 1 then the algorithm can provide suboptimal values. This can be explained by considering the following case. In the proposed optimization algorithm, when the stopping criteria is met, then the current values of $\lambda_(p, i)$, $P_(p, j)$ and $P_(s, i, j)^*$ are used as potential optimal point and the algorithm finds the next potential optimal point by choosing another value of λ_p. Let us consider the following case:

$$P_{OA,s}(\lambda_{p,i0}, P_{p,m}, P^*_{s,i0,m}) > P_{OA,s}(\lambda_{p,i0}, P_{p,n}, P^*_{s,i0,n}) > P_{OA,s}^{stop} \quad \text{for } m > n. \tag{31}$$

In this case the proposed algorithm stops (because of the *Break* command which terminates the inner loop associated with P_p) when it reaches the first optimal point $(\lambda_{p,i0}, P_{p,n}, P^*_{s,i0,n})$ and, it will not scan the next values of $P_{p,i}$. However, there may exist a better point $P_{OA,s}(\lambda_{p,i0}, P_{p,m}, P^*_{s,i0,m})$ at the same spatial density $\lambda_{p,i0}$. Although the proposed algorithm may provide suboptimal solution when $P_{OA,s}^{stop} < 1$ it will provide the optimal solution if we set $P_{OA,s}^{stop} = 1$. This point can be explained as follows. Suppose we have set $P_{OA,s}^{stop} = 1$ and assume that there are k optimal values $[(\lambda^*_{p,1}, P^*_{p,1}, P^*_{s,1}), (\lambda^*_{p,2}, P^*_{p,2}, P^*_{s,2}).(\lambda^*_{p,k}, P^*_{p,k}, P^*_{s,k})]$ of λ_p, P_p, P_s that can achieve $P_{OA,s} = 1$ then the proposed algorithm will terminate at the first such event when $P_{OA,s} = 1$ and will return the corresponding optimal values $(\lambda^*_{p,1}, P^*_{p,1}, P^*_{s,1})$. Now instead, if the algorithm does not stop and search for further optimal values then it will compute optimal values as $[(\lambda^*_{p,1}, P^*_{p,1}, P^*_{s,1}), (\lambda^*_{p,2}, P^*_{p,2}, P^*_{s,2}).(\lambda^*_{p,k}, P^*_{p,k}, P^*_{s,k})]$. The corresponding overall success probability for all of these optimal values will have same value 1 because the probability can not have value greater than 1. Therefore, nothing extra will be achieved in terms of overall success probability by running the algorithm for all the possible values of λ_p, P_p and P_s. It is due to this reason we have putted a *Break* condition to terminate the loop and reduce complexity.

IV. SIMULATION RESULTS

We have performed simulations in MATLAB to obtain the results. The simulation parameters are λ_p, P_p, P_s, λ_s, T_p, T_s, P^p_{suc}, ν and α. The values of different parameters are provided in Table II. The value of transmit power for sensors is chosen according to the transmit power of CC2420 transceivers. In the following we discuss seven types of results. The first three results show that the overall success probability of the sensor network can be optimized with respect to P_s, P_p and λ_p. The following two results show the performance of

TABLE 2. Simulation parameters.

Parameter	Range
P_s	.1 – 1 mW
P_p	.1 – 1 W
λ_s	$5 - 30\ m^{-2}$
λ_p	$.03 - .3\ m^{-2}$
T_p	.25
T_s	.2
P^p_{suc}	.8
ν	1

the sensor network when optimization with respect to these three parameters is performed. Then we compare the overall success probability and throughput of a typical sensor for the proposed optimization scheme with the scheme in [13]. We use $\alpha = 4$ unless otherwise stated.

Fig. 3 shows the overall success probability as a function of sensor transmit power for different values of P_p. It can be observed that for different values of P_p there exists a corresponding optimal P_s for which the overall success probability is maximum. Further, it can be observed that as P_p increases the optimal point shift towards right side. This is because the interference at the nearest IS increases with the increase in P_p and hence higher transmit power is required for the sensors to overcome the effect of interference in the SIR. This results in higher optimal transmit power for the sensors.

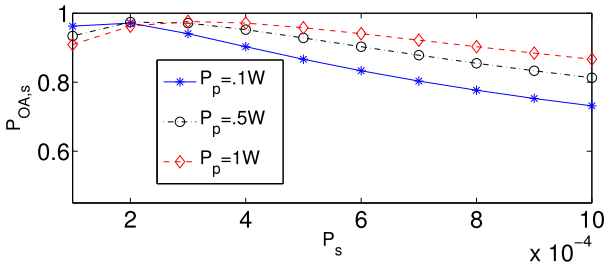

FIGURE 3. Overall success probability as a function of P_s for different values of P_p and $\lambda_p = .1$.

In Fig. 4 we present the overall success probability as a function of P_p for different values of sensor transmit power. The presence of an optimal P_p for different values of P_s can be easily observed from Fig. 4. In this case the optimal transmit power of the AP increases with the increase in P_s. This is because higher transmit powers from the APs increase the received power at the sensor. This in turn increases the harvested energy at the sensor and the energy success probability decreases slowly for higher P_p as compared to smaller P_p. This results in a higher overall success probability for higher P_p. Thus, shifting the optimal point of the P_p to the right side for higher values of P_s. However, if P_p is increased further then the interference contribution at the IS also increases which causes the reduction of transmission success probability and hence we observe the decrease in overall success probability for higher values of P_p.

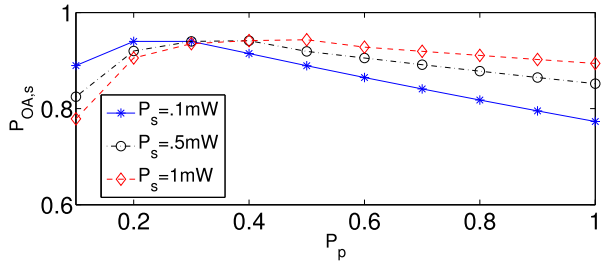

FIGURE 4. Overall success probability as a function of P_p for different values of P_s.

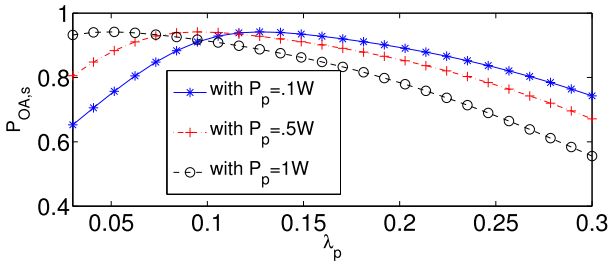

FIGURE 5. Overall success probability as a function of λ_p for different values of P_p and $P_s = .2mW$.

The existence of optimal density of AP for different values of P_p is shown in Fig. 5. The optimal number of AP per unit area increases as the transmit power of the individual AP decreases. The reason for this behavior is the energy success probability of the sensor network. As the transmit power of the AP decrease the probability that a sensor harvest enough energy to be able to transmit decreases and hence the overall success probability also decrease. To overcome this, the density of the APs can be increased which will increase the energy success probability. The increase in λ_p will also increase the interference at the IS which will decrease the transmission success probability. However, for relatively smaller values of λ_p the effect of interference is overcome by the improvement in the energy success probability. Due to these reasons we see that the optimal point of the λ_p moves to right side for smaller P_p.

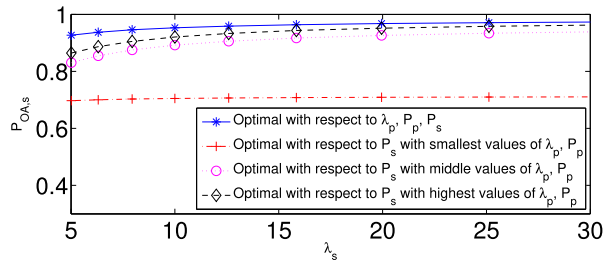

FIGURE 6. Optimized overall success probability as a function of λ_s.

The result of the optimization of overall success probability with respect to P_p, λ_p and P_s is shown in Fig. 6. We have used the algorithm shown in Fig. 2 for performing the optimization. For comparison purposes, we have also shown the results of optimization with respect to P_s with different fixed values of P_p and λ_p. The smallest values of P_p and λ_p refers to .1 watt and .03 m^{-2}, respectively. Similarly highest values refer to $\lambda_p = .3\ m^{-2}$, $P_p = 1$ watt and middle values refer to $\lambda_p = .165\ m^{-2}$, $P_p = .5$ watt. It can be seen that the result for optimizing with respect to all three parameters outperforms the other results. This improvement is due to the increase in number of degrees of freedom available for optimization. Further, we see that the overall success probability increases with the increase in λ_s. This is because with increasing λ_s the distance between a typical sensor and its nearest IS decreases which result in reduced path loss. Hence, the transmission

success probability increases and overall success probability also increases.

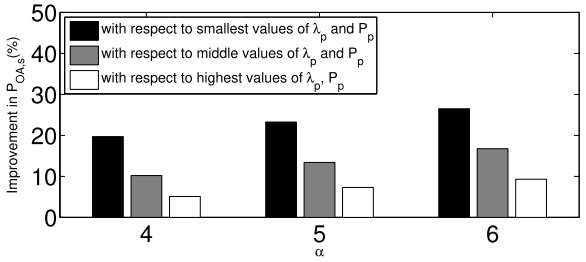

FIGURE 7. **Improvement in overall success probability as a function of α for $\lambda_s = 5$.**

In Fig. 7 we show the improvement in overall success probability for $\alpha = 4, 5, 6$. It can be observed that the improvement increases with increasing α. This is because the optimal values of P_p, P_s and λ_p depends on α. Although highest values of P_p and λ_p are desirable for increasing the energy success probability however these highest values may not be suitable for transmission success probability. In a similar way if the smallest values are chosen for P_p and λ_p then these values are suitable for transmission success probability however they may not be suitable for energy success probability. Therefore, if optimization is performed with respect to all these parameters then performance will be better in comparison to the case when optimization is performed only on the basis of a single parameter.

Now, we compare the overall success probability of the proposed scheme with the scheme in [13]. For comparison, we assume that the D2D cognitive users defined in [13] are the sensors and they harvest energy from the transmissions in the shared primary spectrum only. The transmit power of the sensors is found from the channel inversion power control [13]. In channel inversion power control, the transmit power depends on the distance between the transmitter and receiver. The interested reader can find the details of channel inversion power control in [33, Sec. III-B]. According to [13] the cognitive users, sensors in our case, will transmit only if the average power received from the nearest transmitter is below a certain threshold ω. The overall success probability achieved by scheme in [13] for different values of ω is compared with our proposed scheme in Fig. 8. It can be observed from Fig. 8 that the overall success probability of the proposed algorithm is better than that achieved by [13] for different density of sensors. This improvement can be explained as follows. A particular value of ω will translate into some protection region around the transmitter within which no transmitter of the shared spectrum can be active. This means that a sensor will transmit only if the nearest transmitter of the shared spectrum is out of some protection region and the harvested power is greater than the required transmit power of the sensor. This event, denoted by energy success in our work, becomes less probable with the decrease in ω due to reduction in the received power. This means the energy success probability reduces with decrease in ω. On the other hand the transmission success probability increases due to the reduction in ω. However, the increase in transmission success probability is not sufficient to overcome the reduction in energy success probability. This is because the ω is defined in accordance with the transmitter and not in accordance with the receiver in [13] and the interference at receiver may still be higher even if the interference perceived by the transmitter is small. One other advantage of our scheme is the ability of sensor to transmit. This point can be explained as follows. In [13] a cognitive user will be able to transmit only if there is no active primary transmitter within the protection region. This means that the sensors which are deployed nearby primary transmitter will never be able to transmit according to the scheme of [13]. On the other hand in our scheme the sensors transmit in such a manner so that the outage probability of the primary network is below a certain threshold. In this way, the sensors which are deployed nearby a primary transmitter can also get a chance to transmit their sensed information to nearest IS.

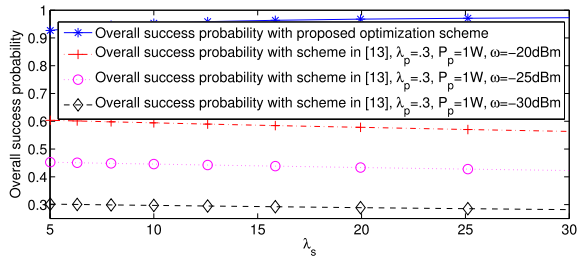

FIGURE 8. **Overall success probability comparison between proposed optimization scheme and [13].**

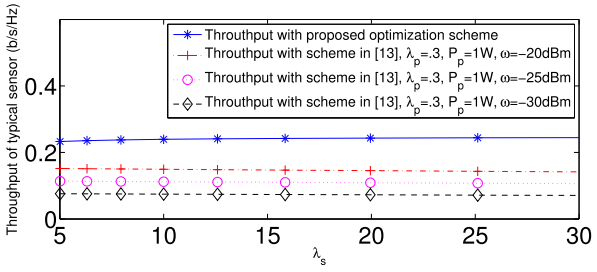

FIGURE 9. **Throughput comparison between proposed optimization scheme and [13].**

In Fig. 9, we have compared the throughput of a typical sensor node for the proposed scheme with the throughput of the scheme proposed in [13]. The throughput is defined as the product of the data rate and the overall success probability. Therefore, throughput can be considered as the overall performance metric of the communication system. The throughput of the proposed scheme is considerably better than that achieved by [13]. The same reasoning that was used to explain the improvement of the overall success probability can be used to explain the improvement of the throughput.

V. CONCLUSIONS

In this paper we have analyzed overall success probability for the energy harvesting and spectrum sharing WSN. It is considered that overall success probability is a product of the transmission success probability and energy success probability. The transmission success probability accounts for channel imperfections and interference effects while energy success probability considers the randomness in the harvested energy. It is shown that transmission success probability increases with increasing P_s and decreases with the increase in λ_p, P_p. However, the energy success probability decreases with increasing P_s and increases with the increase in λ_p, P_p. Therefore, it is concluded that the overall success probability, being a product of transmission success and energy success probabilities, can be optimized with respect to P_s, λ_p and P_p. Based on this conclusion we have proposed an algorithm to perform optimization with respect to P_s, λ_p and P_p. It is shown that considerable improvements in overall success probability can be made by performing optimization over P_s, P_p and λ_p. Simulation results show that the overall success probability and throughput of the proposed scheme are better than those of the existing scheme. We have considered RF energy harvesting therefore our proposed solution for maximizing the overall success probability can also be applied to WSNs that are located in indoor environments. Further, as the optimization can be performed on P_p, P_s, λ_p individually, our solution is therefore also applicable to the scenarios where one or two of these (P_p, P_s, λ_p) parameters are fixed and optimization can be performed on one or two parameters only.

APPENDIX A
THE VALUES OF *A*, *B*, *C* AND *D*

In this appendix we derive the expressions for A and B however similar steps can be carried out to obtain the values of C and D also. We know that

$$A = e^{-2\pi\lambda_p \int_{x_0}^{\infty}\left(\frac{Mx^{-\alpha}}{1+Mx^{-\alpha}}\right)xdx}, \tag{A1}$$

where $M = T_p x_0^{\alpha}$ is used for simplification of notation. By using change of variable with $\frac{x^{\alpha}}{M} = v$ the integral $\int_{x_0}^{\infty}\left(\frac{Mx^{-\alpha}}{1+Mx^{-\alpha}}\right)xdx$ in the above expression can be written as follows

$$\int_{x_0}^{\infty}\frac{x}{1+\frac{x^{\alpha}}{M}}dx = \frac{T_p^{\frac{2}{\alpha}}x_0^2}{\alpha}\int_{\frac{1}{T_p}}^{\infty}\frac{v^{\frac{2}{\alpha}-1}}{1+v}dv. \tag{A2}$$

Now using $\int_u^{\infty}\frac{x^{\mu-1}}{(1+\beta x)^{\nu}}dx = {}_2F_1(\nu, \nu-\mu; \nu-\mu+1; -\frac{1}{\beta u})\left[\frac{u^{\mu-\nu}}{\beta^{\nu}(\nu-\mu)}\right]$[34, eq. 3.194] we can write

$$\int_{x_0}^{\infty}\frac{x}{1+\frac{x^{\alpha}}{M}}dx = {}_2F_1(1, 1-\frac{2}{\alpha}; 2-\frac{2}{\alpha}; -T_p)\frac{x_0^2 T_p}{\alpha-2}. \tag{A3}$$

Now putting (A3) into (A1) we can obtain the value of A as defined in (7). Now we find B. In this case the value of dummy variable $M = T_p\frac{P_s}{P_p}x_0^{\alpha}$ and the lower limit of the integration is 0. By using $\frac{y^{\alpha}}{M} = v$, the integral $\int_0^{\infty}\left(\frac{T_p\frac{P_s}{P_p}x_0^{\alpha}y^{-\alpha}}{1+T_p\frac{P_s}{P_p}x_0^{\alpha}y^{-\alpha}}\right)ydy$ in B can be written as

$$\int_0^{\infty}\left(\frac{T_p\frac{P_s}{P_p}x_0^{\alpha}y^{-\alpha}}{1+T_p\frac{P_s}{P_p}x_0^{\alpha}y^{-\alpha}}\right)ydy = \int_0^{\infty}\frac{y}{1+\frac{y^{\alpha}}{M}}dy = \frac{T_p^{\frac{2}{\alpha}}\frac{P_s}{P_p}x_0^{\alpha}}{\alpha}\int_0^{\infty}\frac{v^{\frac{2}{\alpha}-1}}{1+v}dv, \tag{A4}$$

where the integral $\int_0^{\infty}\frac{v^{\frac{2}{\alpha}-1}}{1+v}dv = \Gamma(\frac{2}{\alpha})\Gamma(1-\frac{2}{\alpha})$ [34, eqs. (3.194) and (8.384)]. Putting (A4) into (8) and using the fact that $\Gamma(1+z) = z\Gamma(z)$ we can obtain the value of B as presented in (9).

It can be easily seen that the integration term $\int_0^{\infty}\frac{T_s y_0^{\alpha}\frac{P_p}{P_s}x^{-\alpha}}{1+T_s y_0^{\alpha}\frac{P_p}{P_s}x^{-\alpha}}xdx$ in C is similar to the integration term of B evaluated above. Therefore, same steps can be carried out again to obtain the result of C presented in (19). In a similar way we can see that integration term $\int_{y_0}^{\infty}\frac{T_s y_0^{\alpha}y^{-\alpha}}{1+T_s y_0^{\alpha}y^{-\alpha}}ydy$ in D is similar to the integration term of A evaluated above. Therefore, same steps can be used to get the result of D presented in (19).

APPENDIX B
CDF OF $P_{h,s}$

The CDF of $P_{h,s}$ for a certain value t is obtained by integrating the inverse Laplace transform of $P_{h,s}$ from 0 to t. It can be observed that our expression for Laplace transform of $P_{h,s}$ (27) is same as the expression provided in [33, eq. (8)] with $\lambda_1 = \lambda_p, \lambda_2 = p_{SA,max}\lambda_s, P_1 = P_p, P_2 = P_s, a = v, K = 2$. Therefore, the CDF of $P_{h,s}$ can be obtained as follows [32, eq. (9)]

$$F_{P_{h,s}}(t) = 1-\int_0^{\infty}\frac{1}{\pi x}e^{-xt-\frac{2\pi^2(vx)^{\frac{2}{\alpha}}\chi}{\alpha\tan\left(\frac{2\pi}{\alpha}\right)}}\sin\left(\frac{2\pi^2(vx)^{\frac{2}{\alpha}}\chi}{\alpha}\right)dx. \tag{B1}$$

The probability that the harvested power is greater than P_s is obtained by $P_{e,s}^{S} = 1 - F_{P_{h,s}}(P_s) = \int_0^{\infty}\frac{1}{\pi x}e^{-xP_s-\frac{2\pi^2(vx)^{\frac{2}{\alpha}}\chi}{\alpha\tan\left(\frac{2\pi}{\alpha}\right)}}\sin\left(\frac{2\pi^2(vx)^{\frac{2}{\alpha}}\chi}{\alpha}\right)dx$.

REFERENCES

[1] I. F. Akyildiz, W. Su, Y. Sankarasubramaniam, and E. Cayirci, "A survey on sensor networks," *IEEE Commun. Mag.*, vol. 40, no. 8, pp. 102–114, Aug. 2002.
[2] Z. Ding, S. M. Perlaza, I. Esnaola, and H. V. Poor, "Power allocation strategies in energy harvesting wireless cooperative networks," *IEEE Trans. Wireless Commun.*, vol. 13, no. 2, pp. 846–860, Feb. 2014.
[3] I. Krikidis, "Relay selection in wireless powered cooperative networks with energy storage," *IEEE J. Sel. Areas Commun.*, vol. 33, no. 12, pp. 2596–2610, Dec. 2015.
[4] A. A. Nasir, X. Zhou, S. Durrani, and R. A. Kennedy, "Relaying protocols for wireless energy harvesting and information processing," *IEEE Trans. Wireless Commun.*, vol. 12, no. 7, pp. 3622–3636, Jul. 2013.

[5] D. S. Michalopoulos, H. A. Suraweera, and R. Schober, "Relay selection for simultaneous information transmission and wireless energy transfer: A tradeoff perspective," *IEEE J. Sel. Areas Commun.*, vol. 33, no. 8, pp. 1578–1594, Aug. 2015.

[6] T. Li, P. Fan, and K. B. Letaief, "Outage probability of energy harvesting relay-aided cooperative networks over rayleigh fading channel," *IEEE Trans. Veh. Technol.*, vol. 65, no. 2, pp. 972–978, Feb. 2016.

[7] N. T. Do, V. N. Q. Bao, and B. An, "Outage performance analysis of relay selection schemes in wireless energy harvesting cooperative networks over non-identical Rayleigh fading channels," *Sensors*, vol. 16, no. 3, pp. 1–19, 2016.

[8] P. N. Son and H. Y. Kong, "Exact outage analysis of energy harvesting underlay cooperative cognitive networks," *IEICE Trans. Commun.*, vols. E98.B, no. 4, pp. 661–672, 2015.

[9] Y. Liu, S. A. Mousavifar, Y. Deng, C. Leung, and M. Elkashlan, "Wireless energy harvesting in a cognitive relay network," *IEEE Trans. Wireless Commun.*, vol. 15, no. 4, pp. 2498–2508, Apr. 2016.

[10] C. Zhai, J. Liu, and L. Zheng, "Cooperative spectrum sharing with wireless energy harvesting in cognitive radio networks," *IEEE Trans. Veh. Technol.*, vol. 65, no. 7, pp. 5303–5316, Jul. 2016.

[11] Z. Wang, Z. Chen, B. Xia, L. Luo, and J. Zhou, "Cognitive relay networks with energy harvesting and information transfer: Design, analysis, and optimization," *IEEE Trans. Wireless Commun.*, vol. 15, no. 4, pp. 2562–2576, Apr. 2016.

[12] Y. Liu, L. Wang, S. A. R. Zaidi, M. Elkashlan, and T. Q. Duong, "Secure D2D communication in large-scale cognitive cellular networks: A wireless power transfer model," *IEEE Trans. Commun.*, vol. 64, no. 1, pp. 329–342, Jan. 2016.

[13] A. H. Sakr and E. Hossain, "Cognitive and energy harvesting-based d2d communication in cellular networks: Stochastic geometry modeling and analysis," *IEEE Trans. Commun.*, vol. 63, no. 5, pp. 1867–1880, May 2015.

[14] F. K. Shaikh and S. Zeadally, "Energy harvesting in wireless sensor networks: A comprehensive review," *Renew. Sustain. Energy Rev.*, vol. 55, pp. 1041–1054, Mar. 2016.

[15] A. González, R. Aquino, W. Mata, A. Ochoa, P. Saldaña, and A. Edwards, "Open-WiSe: A solar powered wireless sensor network platform," *Sensors*, vol. 12, no. 6, pp. 8204–8217, 2012.

[16] M. M. Abbas *et al.*, "Solar energy harvesting and management in wireless sensor networks," *Int. J. Distrib. Sensor Netw.*, vol. 2014, Jul. 2014, Art. no. 436107, doi: 10.1155/2014/436107.

[17] Y. Li and R. Shi, "An intelligent solar energy-harvesting system for wireless sensor networks," *EURASIP J. Wireless Commun. Netw.*, vol. 2015, Jun. 2015, Art. no. 179, doi: 10.1186/s13638-015-0414-2.

[18] D. Niyato, E. Hossain, and A. Fallahi, "Sleep and wakeup strategies in solar-powered wireless sensor/mesh networks: Performance analysis and optimization," *IEEE Trans. Mobile Comput.*, vol. 6, no. 2, pp. 221–236, Feb. 2007.

[19] L. Mateu, C. Codrea, N. Lucas, M. Pollak, and P. Spies, "Energy harvesting for wireless communication systems using thermogenerators," in *Proc. 21st Conf. DCIS*, 2006, pp. 22–24.

[20] Y. K. Tan, K. Y. Hoe, and S. K. Panda, "Energy harvesting using piezoelectric igniter for self-powered radio frequency (RF) wireless sensors," in *Proc. IEEE ICIT*, Dec. 2006, pp. 1711–1716.

[21] H. J. Visser and R. J. M. Vullers, "RF energy harvesting and transport for wireless sensor network applications: Principles and requirements," *Proc. IEEE*, vol. 101, no. 6, pp. 1410–1423, Jun. 2013.

[22] M. Y. Naderi, P. Nintanavongsa, and K. R. Chowdhury, "RF-MAC: A medium access control protocol for re-chargeable sensor networks powered by wireless energy harvesting," *IEEE Trans. Wireless Commun.*, vol. 13, no. 7, pp. 3926–3937, Jul. 2014.

[23] A. Bakkali, J. Pelegri-Sebastia, T. Sogorb, V. Llario, and A. Bou-Escriva, "A dual-band antenna for RF energy harvesting systems in wireless sensor networks," *J. Sensors*, vol. 2016, Jan. 2016, Art. no. 5725836. [Online]. Available: http://dx.doi.org/10.1155/2016/5725836

[24] S. Park, J. Heo, B. Kim, W. Chung, H. Wang, and D. Hong, "Optimal mode selection for cognitive radio sensor networks with RF energy harvesting," in *Proc. IEEE 23rd Int. Symp. PIMRC*, Sep. 2012, pp. 2155–2159.

[25] M. Y. Naderi, K. R. Chowdhury, and S. Basagni, "Wireless sensor networks with RF energy harvesting: Energy models and analysis," in *Proc. IEEE WCNC*, Mar. 2015, pp. 1494–1499.

[26] W. Liu, X. Zhou, S. Durrani, H. Mehrpouyan, and S. D. Blostein, "Energy harvesting wireless sensor networks: Delay analysis considering energy costs of sensing and transmission," *IEEE Trans. Wireless Commun.*, vol. 15, no. 7, pp. 4635–4650, Jul. 2016.

[27] T. Q. Wu and H. C. Yang, "On the performance of overlaid wireless sensor transmission with RF energy harvesting," *IEEE J. Sel. Areas Commun.*, vol. 33, no. 8, pp. 1693–1705, Aug. 2015.

[28] P. V. Mekikis, A. Antonopoulos, E. Kartsakli, A. S. Lalos, L. Alonso, and C. Verikoukis, "Information exchange in randomly deployed dense WSNs with wireless energy harvesting capabilities," *IEEE Trans. Wireless Commun.*, vol. 15, no. 4, pp. 3008–3018, Apr. 2016.

[29] R. Atallah, M. Khabbaz, and C. Assi, "Energy harvesting in vehicular networks: A contemporary survey," *IEEE Trans. Wireless Commun.*, vol. 23, no. 2, pp. 70–77, Apr. 2016.

[30] M. Haenggi, "On distances in uniformly random networks," *IEEE Trans. Inf. Theory*, vol. 51, no. 10, pp. 3584–3586, Oct. 2005.

[31] T. S. Rappaport, "The wireless revolution," *IEEE Commun. Mag.*, vol. 29, no. 11, pp. 52–71, Nov. 1991.

[32] J. G. Andrews, F. Baccelli, and R. K. Ganti, "A tractable approach to coverage and rate in cellular networks," *IEEE Trans. Commun.*, vol. 59, no. 11, pp. 3122–3134, Nov. 2011.

[33] A. H. Sakr and E. Hossain, "Analysis of K-tier uplink cellular networks with ambient RF energy harvesting," *IEEE J. Sel. Areas Commun.*, vol. 33, no. 10, pp. 2226–2238, Oct. 2015.

[34] I. S. Gradshteyn and I. M. Ryzhik, *Table of Integrals, Series, and Products*, 7th ed. San Diego, CA, USA: Academic, 2007.

MATEEN ASHRAF received the B.Eng. and M.S. degrees, in 2010 and 2013, respectively. He is currently pursuing the Ph.D. degree with the Department of Information and Communication Engineering, Sejong University, South Korea.

ADNAN SHAHID (M'15) received the B.Eng. and M.Eng. degrees in computer engineering with specialization in communication from the University of Engineering and Technology, Taxila, Pakistan, in 2006 and 2010, respectively, and the Ph.D. degree in information and communication engineering from Sejong University, South Korea, in 2015. He is currently a Post-Doctoral Researcher with IDLab, Department of Information Technology, University of Ghent–imec, Belgium. He is coordinating and actively involved in the research activities of the research project eWINE funded by European Commission under the Horizon2020 program. From 2015 to 2016, he was with the Department of Computer Engineering, Taif University, Saudi Arabia. In 2015, he was as a Post-Doctoral Researcher with Yonsei University, South Korea. From 2012 to 2015, he was a Ph.D. Research Assistant with Sejong University. From 2007 to 2012, he served as a Lecturer with Electrical Engineering Department, National University of Computer and Emerging Sciences, Pakistan. He was also a recipient of the prestigious BK 21 plus Postdoc Program at Yonsei University. He actively involved in various research activities. He is an Associate Editor of the IEEE Access Journal.

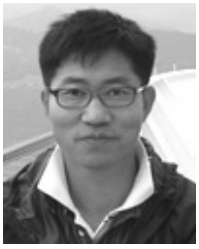

JU WOOK JANG received the B.S. degree in electronic engineering from Seoul National University, Seoul, South Korea, the M.S. degree in electrical engineering from the Korean Advanced Institute of Science and Technology, and the Ph.D. degree in electrical engineering from the University of Southern California, Los Angeles, USA. From 1985 to 1988 and 1993 to 1994, he was with Samsung Electronics, Suwon, South Korea, where he was involved in the development of a 1.5-Mb/s video codec and a parallel computer. Since 1995, he has been with Sogang University, Seoul, where he is currently a Professor. His current research interests include WiMAX protocols, mobile networks, and next-generation networks. He received the LG Yonam overseas research grant in 2001. He has also built systems for video conferencing, streaming, home networks, and ad hoc networks using protocols, such as RTP, SIP, IoT, and blockchain.

KYUNG-GEUN LEE received the B.S. degree in electronics engineering from Seoul National University, in 1981, the M.S. degree in electronics engineering from the Korea Advanced Institute of Science and Technology in 1983, and the Ph.D. degree from the School of Electrical Engineering, Cornell University, Ithaca, NY, USA, in 1992. From 1983 to 1986, and during 1992-1998, he was a Principal Engineer with Network Research Group, Samsung Electronics, South Korea. He is currently a Full Professor with the Department of Information and Communication Engineering, Sejong University, where he was the Director of the Computing and Information Center and Dean of Electrical and Information Engineering College. His research interests include wired and wireless networking, smart buildings and energy harvesting, cognitive radios, and network management.